ANNALS OF GEOPHYSICS, 67, 4, NG444, 2024; doi:10.4401/ag-9182
OPEN ACCESS

Boolean Delay Equations: a dynamical approach to modeling complex systems

Michael Ghil*,1,2,3

(1) Ecole Normale Superieure and PSL University, Department of Geosciences and Laboratoire de Meteorologie Dynamique, Paris, France
(2) University of California at Los Angeles, Department of Atmospheric and Oceanic Sciences, Los Angeles, USA
(3) Imperial College, Department of Mathematics, London, UK

Article history: received October 10, 2024; accepted October 16, 2024

Abstract

Boolean delay equations (BDEs) are equations with discrete variables evolving in continuous time. They serve as exploratory tools in the study of nonlinear and complex systems. In this review paper, we outline their formulation and illustrate their properties by application to a solid-earth problem and a climate one. The first problem is the seismotectonic description and prediction of earthquakes and of their clustering. The second one is that of the coupled atmosphere-ocean phenomenon of the El Niño-Southern Oscillation (ENSO). Both involve irregular behavior that is hard to predict, although some form of cyclicity is present in both, especially in ENSO. The paper concludes with broad perspectives on the further use of BDEs in the geosciences and elsewhere.

Keywords: Boolean Delay Equations; Complex Systems; Earthquake; ENSO; Tipping Points

1. Introduction and motivation

Characterizing and predicting the dynamics of geophysical systems – such as Earth's crust and its earthquakes or the coupled atmosphere-ocean system and its El Niño-Southern Oscillation (ENSO) – is a major challenge due to their inherent nonlinearity and complexity, as well as to the presence of multiple scales of motion and interacting processes (Ghil, 2001; Ghil and Lucarini, 2020; Newman et al., 1994). Despite advances in observational technologies and theoretical frameworks, both types of phenomena remain difficult to forecast with high precision, particularly over long timescales that exceed their intrinsic ones.

Traditionally, different approaches have been used to understand and forecast the behavior of such systems. In the case of earthquakes (Keilis-Borok, 2002), models are often derived from historical data, seismic wave propagation analysis, and fault dynamics, using statistical methods like the Gutenberg-Richter law and the concept of seismic cycles (Keilis-Borok and Shebalin, 1999; Turcotte et al., 2000). For ENSO, climate scientists rely heavily on coupled ocean-atmosphere models (Neelin et al., 1994), using sea surface temperature (SST) and wind patterns to predict its phases – namely, El Niño, La Niña, and neutral – and their amplitudes. These models range over an entire hierarchy, from the simplest conceptual ones that emphasize basic understanding to the most detailed ones that emphasize comprehensiveness and the best possible match to observations (Schneider and Dickinson, 1974; Ghil, 2001; Held, 2005).

A unifying view of the models across such a hierarchy is that of dynamical systems theory. A dynamical system consists of a set of rules that describe how a state of the system evolves over time (Schuster, 1988). In mathematical terms, this evolution is most often expressed through ordinary or partial differential equations (ODEs or PDEs for short), which determine the future state of the system for all times, given its current state. Dynamical systems have proven to be a useful abstraction for modeling various geophysical systems (Ghil and Childress, 1987; Dijkstra and Ghil, 2005) due to their ability to describe the nonlinear, chaotic, and often intermittent behavior observed in phenomena like earthquakes and ENSO. In this framework, the system is thought of as evolving through different states which can capture cycles, like the recurrence of large earthquakes on a fault, or transitions between different phases, like El Niño, the warm phase, and La Niña, the cold one, in the ENSO phenomenon.

A relatively novel class of dynamical system that has been used in modeling geophysical processes is Boolean Delay Equations (BDEs). BDEs represent the system's state using binary variables – e.g., "on" or "off," "active" or "inactive" – and describe the system's evolution using delays (Dee and Ghil, 1984; Mullhaupt, 1984), which allow a parsimonious description of memory effects (Ghil and Mullhaupt, 1985; Ghil et al., 2008). Early applications have included Quaternary glaciation cycles (Ghil et al., 1987), ENSO regime shifts (Saunders and Ghil, 2001), and earthquake clustering and prediction (Zaliapin et al., 2003b, 2003a).

Unlike classical ODE and PDE models, which use continuous variables to depict the model's state space and differentiation in time to propagate the state, BDEs focus on the time evolution of discrete-valued states in discrete steps. Unlike cellular automata that also use discrete-valued states (Gutowitz, 1991; Wolfram, 1994), though, BDEs do not require all delays to be equal, so that the state is only defined at integer multiples of the common delay, say $t_n = n\Delta t$, and jumps in the state can occur at any moment in time, thus allowing for greater complexity, as we shall see in the next section.

These delays can correspond to characteristic time intervals in physical processes, such as stress accumulation on seismic faults or delayed ocean-atmosphere feedbacks in ENSO. The BDE framework offers a parsimonious, computationally efficient way to model the qualitative behavior of such a system.

BDEs thus provide a robust modeling framework designed to capture the essence of systems characterized by threshold behavior, multiple feedback loops, and distinct time delays (Dee and Ghil, 1984; Ghil and Mullhaupt, 1985; Ghil et al., 1987). In the hierarchical modeling paradigm (Schneider and Dickinson, 1974; Ghil, 2001; Held, 2005), simple conceptual models play a crucial role in hypothesis generation and isolating core mechanisms, while more detailed models seek to simulate these mechanisms more realistically and compare the outcomes with observations (Ghil and Robertson, 2000). In this setting, BDEs can serve as the simplest representations of the fundamental physical processes at play. Furthermore, results obtained through BDEs often highlight phenomena not yet uncovered by conventional modeling tools (Saunders and Ghil, 2001; Zaliapin et al., 2003b, 2003a). BDEs are thus able to suggest mechanisms that can be further examined using more comprehensive models once their basic signatures have been identified.

The growing interest in complex systems, spanning fields from microbiology and economics to the climate sciences and the study of human civilizations, has led to the increasing use of Boolean and other discrete models (Cowan et al., 1994; Gutowitz, 1991; Wolfram, 1994; Kauffman, 1995; Gagneur and Casari, 2005). These models, including BDEs, are being explored intensively due to their ability to simplify intricate problems while maintaining essential features of the dynamics.

In this review paper, we first recall the basic concepts and features of BDEs in Section 2, and then provide two examples of application to earthquakes and ENSO dynamics, in Sections 3 and 4, respectively. Finally, in Section 5 conclusions on BDEs and perspectives for their further in geophysical systems are also discussed.

2. Formulation of BDEs and key properties

The reader interested mostly in applications may proceed at this point to Sections 3 and 4, and return to this section as needed.

2.1 Formulation of BDEs

Consider a system with n continuous state variables, $v = (v_1, v_2, \ldots, v_n) \in \mathbf{R}^n$, each of which has a corresponding natural threshold $q_i \in \mathbf{R}$. For each continuous variable v_i, we define an associated Boolean variable $x_i \in \mathbf{B} = \{0, 1\}$,

representing whether the state is "off" (0) or "on" (1), based on whether v_i is below or above its threshold q_i:

$$x_i = \begin{cases} 0, & v_i \le q_i \\ 1, & v_i > q_i \end{cases} \tag{1}$$

The time evolution of the Boolean variables $x = (x_1, x_2, \ldots, x_n)^T \in \mathbf{B}^n$ is governed by delayed interactions between these variables. A general BDE system is written as

$$\begin{cases} x_1(t) = f_1\big(t, x_1(t-\theta_{11}), x_2(t-\theta_{12}), \cdots, x_n(t-\theta_{1n})\big), \\ x_2(t) = f_2\big(t, x_1(t-\theta_{21}), x_2(t-\theta_{22}), \cdots, x_n(t-\theta_{2n})\big) \\ \qquad\qquad \vdots \\ x_n(t) = f_1\big(t, x_1(t-\theta_{n1}), x_2(t-\theta_{n2}), \cdots, x_n(t-\theta_{nn})\big) \end{cases} \tag{2}$$

here each Boolean variable x_i at time t depends on the delayed values of itself and of the other variables. The functions f_i: $\mathbf{B}^n \to \mathbf{B}$ describe logical interactions using operators like AND, OR, and NOT, while the delays $\theta_{ij} \in \mathbf{R}$ represent the time it takes for changes in x_j to affect x_i. The most common Boolean operators, used herein, are defined in Table 1.

Mathematical symbol	Engineering symbol	Name	Description
$\bar{x}$ or $\neg x$	NOT x	Negator	Not true when x is true
$x \vee y$	x OR y	Logical or	True when either x or y or both are true
$x \wedge y$	x AND y	Logical and	True when both are true
$x \nabla y$	x XOR y	Exclusive or	True only when x and y are not equal
$x \Delta y$		Inclusive and	True only when x and y are equal

Table 1. Common Boolean operators with corresponding description.

BDEs are semi-discrete dynamical system, where the state variables are discrete, while time is treated as continuous. Due to their simplicity and ability to capture essential temporal features, BDEs have found applications in a variety of fields, from biology and epidemiology to engineering and geophysics (Cowan et al., 1994; Gutowitz, 1991; Wolfram, 1994; Kauffman, 1995; Gagneur and Casari, 2005). In geophysical systems, where time delays and thresholds often play a significant role, BDEs offer a useful approach to understanding phenomena that are both nonlinear and complex.

2.2 Key properties of BDEs

BDEs share certain properties with the more familiar class of delay-differential equations (DDEs) (Hale, 1971; Ghil et al., 2015). Most importantly, the initial value problem for either class of dynamical systems requires one to define initial data not just at a point but over an initial interval, the length of which is equal to that of the longest delay involved. In the BDE case of Eq. (2), this is equal to $\{\max \theta_{ij} : 1 < i, j \le n\}$. DDEs, though, can be classified, along with ODEs and DDEs, as differentiable dynamical systems (DDSs).

Consider now for simplicity the scalar case of a Boolean function $x(t)$ that is equal to either 0 or 1 over successive segments of the positive real line $t \in \mathbf{R}+ \equiv \{t \ge 0\}$. Given such initial data over the initial interval $\{0 \le t \le 1\}$, where

we take $max_i\{\theta_i\} = 1$ without loss of generality, the solution of Eq. (2) exists and is unique for all $t \geq 0$. The distance between two solutions $x(t)$ and $y(t)$ with such initial data is given

$$d(x, y) \equiv \int_0^1 |x(t) - y(t)|\, dt \tag{3}$$

and it is called the Hamming distance in coding theory.

Theorem 2.1 ("Pigeon-hole" lemma) *All solutions of Eq. (2) with rational delays only are eventually periodic.*

Remark. By "eventually" we mean that a finite-length transient may occur before periodicity sets in. A transient is an initial state that is only visited once in the evolution of the system along a particular orbit in phase space. An interesting feature of BDEs vs. DDSs in general is precisely that such a transient has finite rather than infinite duration, i.e., asymptotic behavior is reached in finite time. The name of pigeon-hole lemma comes from the fact that – when the delays in Eq. (2) are rational and, necessarily, their number is finite – one can take the least common denominator thereof, say K, so that the number of intervals on which the solutions are constant and equal to either zero or one is, at most, 2^K, so that each solution can be pigeon-holed into one of these concatenations of zeroes and ones.

2.3 Classification of BDEs

Based on the pigeon-hole lemma, and therefore on the behavior for rational delays, one can classify BDE systems as follows (Ghil and Mullhaupt, 1985). All systems with solutions that are immediately periodic, for any piecewise constant initial data, are conservative. All other systems are dissipative and will exhibit, at least for some initial data, transient behavior before settling into eventual periodicity or quasi-periodicity. The DDS analogs are conservative or Hamiltonian dynamical systems (Guckenheimer and Holmes, 1997; Lichtenberg and Liebermann, 1992) vs. forced-dissipative systems, e.g., the well-known Lorenz (1963) system. Typical examples of conservative systems occur in celestial mechanics (Arnol'd, 1978; Varadi et al., 2003), while dissipative systems are often used in modeling geophysical (Ghil and Childress, 1987; Dijkstra and Ghil, 2005) and many other natural phenomena.

The simplest examples of a conservative and dissipative BDE are

$$x(t) = \bar{x}(t-1), \tag{4a}$$

$$x(t) = x(t-1) \wedge x(t-\theta), 0 < \theta < 1 \tag{4b}$$

respectively. The Boolean operators listed in Table 1 include the unary conservative operator $\neg$ (NOT) and two binary ones, $\triangledown$ and $\triangle$ (XOR and its opposite, exclusive AND), as well as two dissipative binary operators, $\vee$ and $\wedge$ (OR and AND). It is common to call a Boolean function $f = (f_1, ..., f_n)$ a connective and its arguments x_i channels (Arnold, 1962); one also refers to a channel x_i simply as channel i.

It is easy to check by hand that, no matter what the piecewise constant distribution of 0's and 1's in the initial interval, the solution of Eq. (4a) is purely periodic, while that of (4b) will become identically equal to 0 in finite time. Likewise, replacing $\wedge$ by $\vee$ Eq. (4b) will eventually, in the precise sense defined above, become identically equal to 1. More generally, a system of BDEs that contains only the conservative operators in its connectives and has only rational delays will become immediately periodic, while dissipative connectives will entail finite transients.

2.4 Unbounded growth in complexity and its approximation

So far, we have only encountered, immediately or eventually, constant or periodic solutions of BDEs. We do not intend here to go into their full theory, but still have to highlight a striking property. Already Dee and Ghil (1984)

noticed that certain BDEs exhibit an unbounded increase in time of the jump function

$$J(t) = \#\{jumps\ of\ x(t)\ within\ the\ interal\ [t, t+1)\} \tag{5}$$

A simple example of this property is given by the scalar conservative BDE

$$x(t) = x(t-1)\nabla x(t-\theta) \tag{6}$$

for any irrational $0 < \theta < 1$. The jump function for $\theta = \theta^* = \sqrt{5} - 1/2$ and a single jump in the initial data on the interval $0 \le t < 1$ is shown in Fig. 1. The delay θ^* is called the "golden ratio": it is well known at least since the Renaissance and already mentioned by Euclid in 300 BCE; θ^* is the most irrational number in the sense that its continued-fraction expansion has the slowest possible convergence (Khinchin, 1964).

Overall, though, the behavior in Fig. 1 is to be expected since the irrational numbers are pervasive on the real line: their measure, i.e., the probability of "meeting" them in any unit interval on the real line, equals 1. In fact, Dee and Ghil (1984) stumbled upon this property totally by accident. What is striking in the figure, is that the growth is not just unbounded but also log-periodic (Ghil and Mullhaupt, 1985), a property of some interest in two areas as diverse as econophysics and antenna arrays.

The unbounded growth of the jump function $J(t)$ for conservative BDE systems would make them an excellent tool in modeling increase of complexity in many areas, such as the striking increase in number of events on the geological time scale, i.e., the "calendar" of events in Earth history, as shown in Fig. 2. A similar increase is recorded in human history (not shown) and many other processes. One may ascribe a portion of this acceleration across many fields of human knowledge to the increase in the number of data available for more recent times, but not all.

On the other hand, one might ask why should this log-periodic increase in the jump function depend crucially on the delays involved in the model being irrational? Well, it actually does not. The Periodic Approximation Theorem below explains why not.

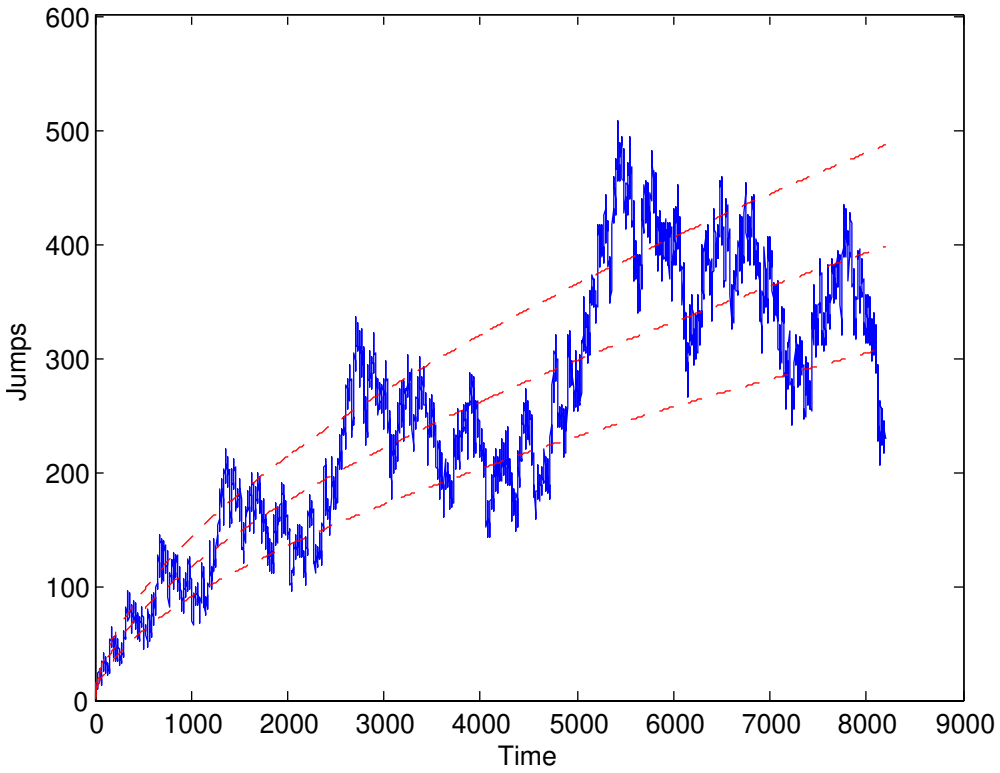

Figure 1. Jump function J(t) for the particular solution of a conservative BDE with the irrational delay $\theta = \theta^* = \sqrt{5} - 1/2$ as in Eq. (6). Adapted from Mullhaupt (2008).

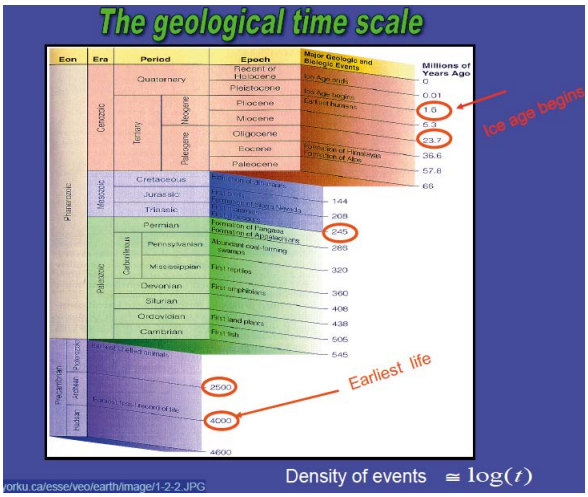

Figure 2. Logarithmic increase in the frequency of events on the geological time scale.

Theorem 2.2 (Periodic approximation) *All solutions to systems of BDEs can be approximated arbitrarily well, with respect to the Hamming norm, for a given finite time, by the periodic solutions of a nearby system that has rational delays only*.

The apparent paradox is thus solved by considering the length of the period obtained for a given conservative BDE and a given rational delay. As the lowest com mon denominator of rational delays becomes larger and larger, the solution in Fig. 1 here is well approximated for longer and longer times, cf. Ghil and Mullhaupt (1985, Fig. 9); i.e., the jump function can grow for a longer time, before periodicity forces it to decrease and return to a very small number of jumps per unit time.

The approximation theorem above, combined with the fact that the probability of chancing upon an irrational number in any unit interval equals 1, makes this BDE property of increasingly complex behavior in time quite useful.

2.5 Normal forms and asymptotic simplification

To study in greater depth dissipative BDEs, Ghil and Mullhaupt (1985) concentrated on the scalar nth-order BDE

$$x(t) = f[x(t-\theta_1), \cdots, x(t-\theta_n)] \tag{7}$$

The connective f is most conveniently expressed in its *normal form* from switching and automata theory, with $xy = x \wedge y$ and $x + y = x \vee y$.

In this notation, the *disjunctive* and *conjunctive* normal forms represent f as a sum of products and a product of sums, respectively. This formalism helps prove that certain BDEs of the form (7) lead to *asymptotic simplification*, *i.e.*, after a finite transient, the solution of the full BDE satisfies a simpler BDE. An illustrative example is

$$x(t) = x(t-\theta_1)\bar{x}(t-\theta_2) \tag{8}$$

where either θ_1 or θ_2 can be larger of the two. Asymptotically, the solutions of Eq. (8) are given by those of a simpler equation

$$x(t) = x(t-\theta_1)\,. \tag{9}$$

Comparison with the asymptotic behavior of forced-dissipative systems in the DDS framework shows two advantages of BDEs. First, the asymptotic behavior sets in after finite, rather than infinite, time. Second, the behavior on the "inertial manifold" or "global attractor" here can be described explicitly by a simpler BDE, while this is rarely the case for a system of ODEs, PDEs, or FDEs.

Finally, one can study asymptotic stability of solutions in the Hamming metric. We conclude this theoretical section by recalling that, for $0 < \theta < 1$ irrational, the solutions of

$$x(t) = x(t-\theta)x(t-1) \tag{10}$$

are eventually equal to $x(t) \equiv 0$, except for $x(t) \equiv 1$, which is unstable. Likewise, for

$$x(t) = x(t-\theta) + x(t-1), \tag{11}$$

$x(t) \equiv 1$ is asymptotically stable, while $x(t) \equiv 0$ is not. More generally, one has the following

Theorem 2.3 *Given rationally unrelated delays* $\{\theta_k : k = 1, \cdots, n\}$*, the BDE*

$$x(t) = \prod_{k=1}^{n} x(t-\theta_k), \tag{12}$$

has $x(t) \equiv 0$ *as an asymptotically stable solution, while for the BDE*

$$x(t) = \sum_{k=1}^{n} x(t-\theta_k), \tag{13}$$

$x(t) \equiv 1$ *is asymptotically stable.*

To complete the taxonomy of solutions, we also note the presence of *quasi-periodic* solutions; see Ghil and Mullhaupt (1985, Eq. (6.18)) and its discussion.

2.6 Asymptotic behavior

In summary, BDE systems have the following types of asymptotic behavior

a) fixed point – the solution reaches one of a finite number of possible states and remains there;
b) limit cycle – the solution becomes periodic;
c) quasi-periodicity – the solution is a sum of several incommensurable "modes";
d) growing complexity – the solution's number of jumps $J(t)$ per unit time increases with time. This number grows like a positive, but fractional power of time t (Dee and Ghil, 1984; Mullhaupt, 1984), with superimposed log-periodic oscillations (Ghil and Mullhaupt, 1985).

We refer for technical details and for further interesting properties of BDEs to Ghil et al. (2008) and to references therein.

3. Seismicity and earthquake clustering

Seismicity has long been modeled through lattice models (Burridge and Knopoff, 1967; Allègre et al., 1982; Bak et al., 1988) that capture key earthquake dynamics like the seismic cycle and the Gutenberg-Richter relation, as well as clustering in space and time (Keilis-Borok, 1996; Scholz, 2002; Turcotte, 1997). A BDE framework can

further simplify the interactions present in these models by focusing on delayed state transitions between loading and unloading and between intact and failed elements (Zaliapin et al., 2003a, 2003b), while still reproducing many of the same key features of earthquake dynamics, as well as important premonitory seismicity patterns (PSPs) that may precede a major earthquake.

Colliding-cascade models (Zaliapin et al., 2003a, 2003b; Gabrielov et al., 2000; Gabrielov et al., 2000) are classical DDS models integrating three key processes that are significant in lithospheric dynamics, namely a hierarchical system structure, continuous external loading forces, and element failures; the latter redistribute load and strength across the system. The model's hierarchical structure corresponds to fault networks, the loading represents tectonic forces, and the failures mimic earthquakes. By incorporating the BDE approach into the colliding-cascade models, one replaces the complex, elementary interactions of system components with their collective effects.

The model operates on a directed ternary graph, in which each node, except the top and the bottom ones, connects to six others; see Zaliapin et al. (2003b, Fig. 1). Every node, except those at the lowest level, serves as the parent to three sibling nodes, while each element is characterized by a degree of *weakness* or *fatigue*, failing when this weakness exceeds a specific threshold. The state of each element is classified via two Boolean functions (s, ℓ):

- $s_e(t) = 0$ if the element is intact, and $s_e(t) = 1$ if it has failed,
- $\ell_e(t) = 0$ if the element is unloaded, and $\ell_e(t) = 1$ if it is loaded.

Element transitions between states occur due to interactions with neighboring elements or due to external forces, subject to time delays between the causal impact and the resulting state transition. Four basic time delays are introduced:

- Δ_L, the delay between the application of load and the transition to a loaded state, $(\cdot, 0) \to (\cdot, 1)$;
- Δ_F, the delay between increasing weakness and failure, $(0, \cdot) \to (1, \cdot)$;
- Δ_D, the delay between failure and unloading, $(\cdot, 1) \to (\cdot, 0)$; and
- Δ_H, the delay between healing and the transition to an intact state, $(1, \cdot) \to (0, \cdot)$.

Initially, at $t = 0$, all elements are in state (0, 0), intact and unloaded. Most state transitions follow the cycle:

$$(0, 0) \to (0, 1) \to (1, 1) \to (1, 0) \to (0, 0) \ldots$$

The model produces a catalog of earthquakes that represent element failures and are similar to real earthquake catalogs:

$$\mathrm{C} = (t_k, m_k, h_k), k = 1, 2, \ldots, t_k \leq t_{k+1}. \tag{9}$$

Here t_k is the time of the rupture, m_k the earthquake magnitude, and h_k the hypocenter location. In the BDE model, earthquakes correspond to element failures, m_k is the hierarchical level of the failed element in the ternary digraph, and its position on that level corresponds to h_k.

The seismic BDE model's solutions were analyzed in terms of the density $\rho(t)$ of elements in a failed state and of the irregularity $G(t)$ of the energy release; see Zaliapin et al. (2003b) for the exact definitions. In terms of these functionals of the states, the model generates synthetic sequences that fall into three seismic regimes:

- Regime **H**: *High and nearly periodic seismicity* (Fig. 3a, magenta domain).
- In this regime, each cycle of fractures reaches the top level, $m = L$, of the ternary graph (depth $L = 6$). The sequence exhibits near-periodicity in a statistical, cyclo-stationary sense (Mertins, 1999).
- Regime **I**: *Intermittent seismicity* (Fig. 3a, blue domain). Seismicity reaches the top level in some but not all cycles, and the cycle duration is highly irregular.
- Regime **L**: *Medium or low seismicity* (Fig. 3a, yellow domain). No cycle reaches the top level, and seismic activity remains more constant at low or medium levels, with fewer prolonged quiescent intervals compared to Regimes **H** and **I**.

Remarkably, the regimes in Fig. 3a have sharp boundaries and a triple point.

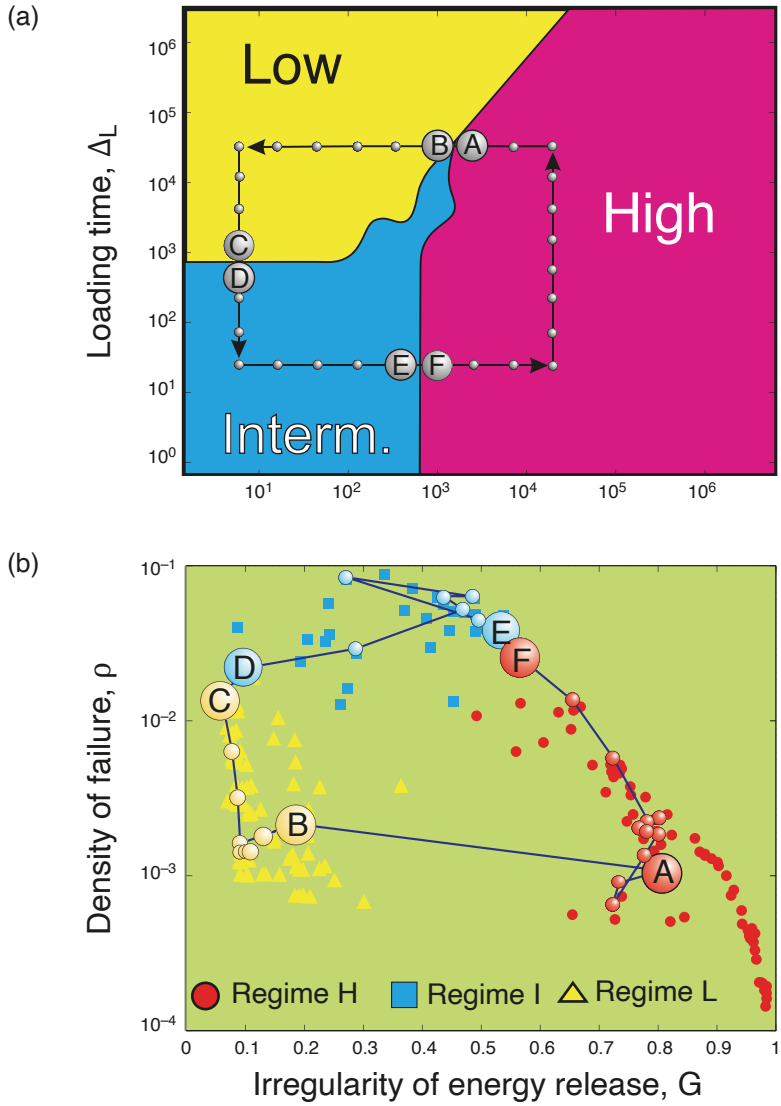

Figure 3. Regime diagram for the BDE seismic model: (a) rectangular path in the delay plane (Δ_L, Δ_H), and (b) the measures G and ρ, calculated along the rectangular path shown in panel (a). The transition between points (A) and (B), i.e., between regimes H and L, is very sharp with respect to the change in irregularity G of energy release, while almost negligible with respect to the change in failure density ρ. The colored circles, triangles, and squares in panel (b) correspond to synthetic catalogs from regimes H, I, and L, respectively. Reproduced from Ghil et al. (2008), with the kind permission of Elsevier.

The changes in failure density $\rho(t)$ and irregularity G were computed for synthetic sequences that correspond to the 30 marked points on the rectangular path in Fig. 3a, as well as for all the points on a uniform grid covering the domain of the figure at the same resolution in $\log \Delta_L$ and $\log \Delta_H$. In Fig. 3b, the closed path $A \to B \to C \to D \to E \to F \to A$ is plotted in the coordinates (Δ_L, Δ_H).

Points A and B straddle the triple point in panel (a) and the jump from A to B is marked by a sharp drop from 0.8 to 0.18 in G, signaling a transition from highly irregular to almost uniform energy release between Regimes **H** and **L**. Interestingly, this shift has little effect on the average failure density ρ. The transitions between the remaining regime pairs are more gradual. Clustering decreases further, from $G = 0.18$ to approximately 0.1, and remains low within Regime **L**. Conversely, between points C and a, G increases steadily, though nonmonotonically, from 0.1 to 0.8 as the system passes through regimes **I** and **H**. As Δ_L increases between points F and A, the average density ρ decreases slightly, while G increases moderately, from 0.5-0.6 to around 0.8. The other points in Fig. 3b shows the coherence of failure density $\rho(t)$ and irregularity of energy release G over the three regimes.

Zaliapin et al. (2003a) explored the application of these findings to earthquake prediction. They utilized simulated catalogs to investigate the effectiveness of pattern recognition methods previously tested on real earthquake catalogs and on other models (Keilis-Borok, 2002; Keilis-Borok and Malinovskaya, 1964; Jaume and Sykes, 1999; Keilis-Borok, 1994; Pepke et al., 1994; Molchan et al., 1990; Knopoff et al., 1996; Bufe and Varnes, 1993; Bowman et al., 1998). Specifically, the seismic BDE model above, when applied to earthquake prediction, focuses on small disturbances in the system that can trigger a cascade of events, ultimately resulting in a major earthquake. These transitions are analogous to large seismic events that occur after prolonged stress accumulation.

The seismic BDE model describes critical transitions that are due to the interaction between direct cascades of loading and inverse cascades of failures in a hierarchical system. This interaction is controlled by distinct delays between switching of elements from one state to another: loaded vs. unloaded and intact vs. failed. The model exhibits four major types of PSPs, which have been previously identified in seismic observations: (i) rise of earthquake clustering; (ii) rise of the earthquakes' intensity; (iii) rise of the spatial correlation range; and (iv) certain changes in the size distribution of earthquakes, i.e., in the Gutenberg-Richter relation. The model exhibits, furthermore, new features of individual PSPs and of their collective behavior, which have to be tested in turn on observations. There are indications that the premonitory phenomena considered are not seismicity-specific, but may be common to hierarchical systems of a more general nature.

4. ENSO variability and paleoclimate

The application of BDEs to the climate sciences started with paleoclimatic studies. Ghil et al. (1987) used BDEs for exploratory purposes, focusing on the coupling between Earth's radiation balance, continental ice sheet mass balance, and the ocean's thermohaline circulation during glaciation cycles. On shorter timescales, Darby and Mysak (1993), as well as Wohlleben and Weaver (1995), explored the coupling between sea ice, atmospheric circulation, and the ocean in the Arctic and North Atlantic's interdecadal climate cycles. In this section, we present a BDE application to ENSO coupling between the Tropical Pacific and the global atmosphere. ENSO is the most significant mode of seasonal-to-interannual climate variability. Known for centuries by South American fishermen, who observed sporadic warming of the cold, nutrient-rich coastal waters, it leads to detrimental impacts on fish harvests. This warming near the coast of Peru became known as El Niño, referring to the "Christ child" due to its tendency to peak near Christmas (Diaz and Markgraf, 1993; Philander, 1990). Starting in the 1970s, the climatic effects of El Niño were found to extend well beyond the Peruvian coast (Diaz and Markgraf, 1993; Glantz et al., 1991; Maraun and Kurths, 2005), prompting global efforts to improve predictions of extreme El Niño events (Latif et al., 1994; Ghil and Jiang, 1998).

The BDE model for ENSO variability is based on three key conceptual elements:

- *Air-sea interaction*: a positive feedback in the Tropics that initiates a chain reaction where initial SST warming in the eastern Pacific weakens the Walker circulation. This weakening leads to westerly wind anomalies, further enhancing SST warming through changes in ocean circulation, thereby closing the feedback loop.
- *Delayed oceanic wave adjustments*: a negative feedback restores colder conditions in the eastern basin. During the warm phase of ENSO, westerly wind anomalies generate a Kelvin wave that propagates eastward, deepening the thermocline and amplifying the warm event. Meanwhile, westward-propagating Rossby waves reflect off the western boundary and create a cooling Kelvin wave that contributes to a switch to the cold, La Niña phase.
- *Seasonal forcing*: resonances between ENSO and the annual cycle (Chang et al., 1994, 1995; Jin et al., 1994, 1996; Tziperman et al., 1994, 1995; Ghil and Robertson, 2000) likely contribute to ENSO events peaking in boreal winter and explain the system's mixture of regularity and irregularity. The BDE model assumes that this seasonal cycle provides a seasonally varying amplification potential.

The model (Saunders and Ghil, 2001) operates using five Boolean variables: the state of the ocean is represented by SST anomalies through two Boolean variables, T_1 and T_2; atmospheric conditions are described by U_1 and U_2, which represent the state of the trade winds; while the seasonal cycle is modeled as a two-level Boolean variable, S. The first variable in each pair, T_1 or U_1, denotes the anomaly's sign, while the second variable, T_2 or U_2, describes its amplitude. The atmospheric variables U_i are "slaved" to the oceanic variables T_i. The evolution of T_1, representing the sign of SST anomalies, is determined by two sets of delayed interactions:

(i) extreme wind stress anomalies generate a Rossby wave signal, $R(t)$, which re-enters the system after a delay τ. Upon arrival in the eastern Pacific, the signal reverses the sign of T_1.

(ii) When $R(t) = 0$, $T_1(t + \tau)$ responds directly to local atmospheric conditions with a delay β, consistent with the Bjerknes (1969) hypothesis.

The model's two key parameters are the delays β and τ, which represent local and basin-wide adjustment processes, respectively. Wind changes lag behind SSTs by β, while τ varies from one month to two years, namely the timescale for oceanic adjustments (Jin, 1996).

In the BDE model, the ENSO phenomenon is primarily characterized by the dynamics of SST states, which are represented by the two-variable Boolean vector (T_1, T_2). Specifically, the four-level scalar variable ENSO is handled by the following set of values of T_1 and T_2.

Throughout our simulations, this variable alternates between the value exactly in this sequence, thereby simulating the real cycles of ENSO. These cycles follow the same order of states, although the time spent within each state varies depending on τ for a fixed β. By defining the period P of a simple oscillatory solution as the interval between the initiation of two consecutive extreme warm events, when ENSO = 2, it is possible to classify the various model solutions; see Figs. 4 and 5.

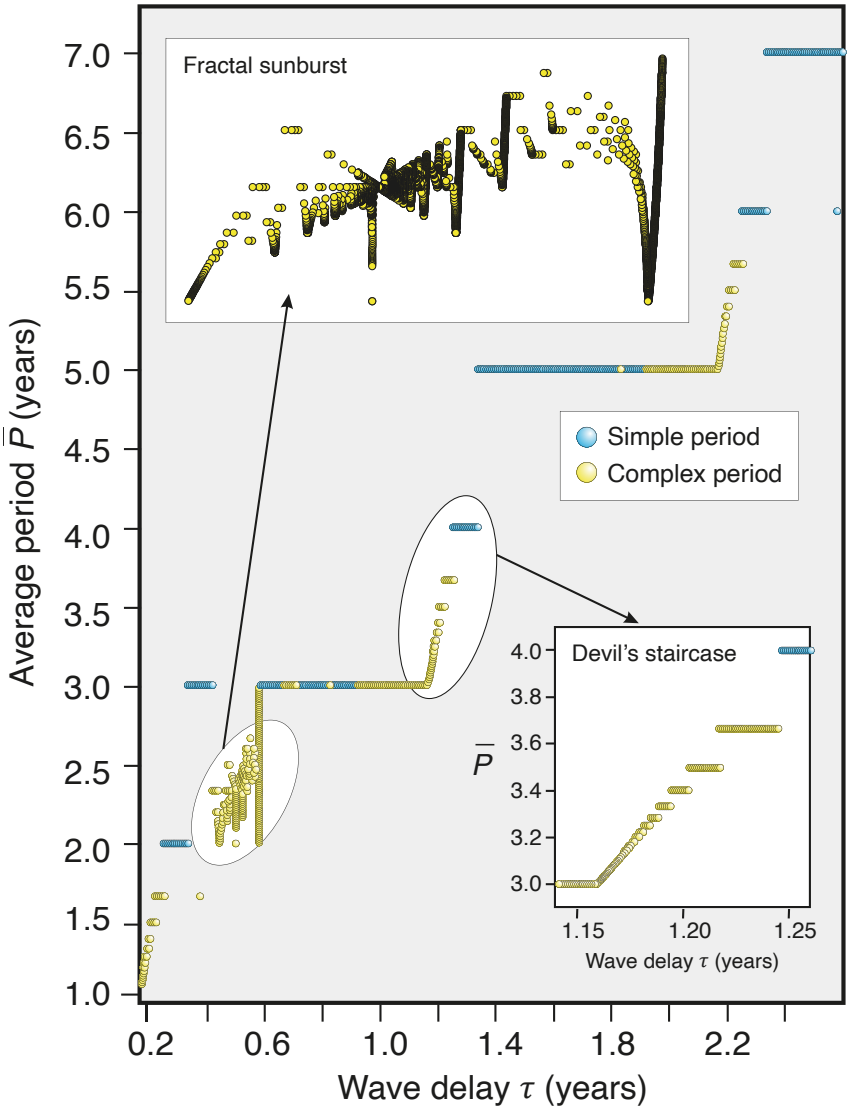

Figure 4. Devil's staircase and fractal sunburst for a BDE model of the ENSO phenomenon. Plotted in the bifurcation diagram is the average cycle length $\overline{P}$ vs. the wave delay τ for a fixed local delay $\beta = 0.17$. Blue dots indicate purely periodic solutions, orange dots are for complex periodic solutions, and small black dots denote aperiodic solutions. The two insets show a blowup of the overall, approximate behavior between periodicities of two and three years ("fractal sunburst") and of three and four years ("Devil's staircase"). Modified after Saudners and Ghil (2001).

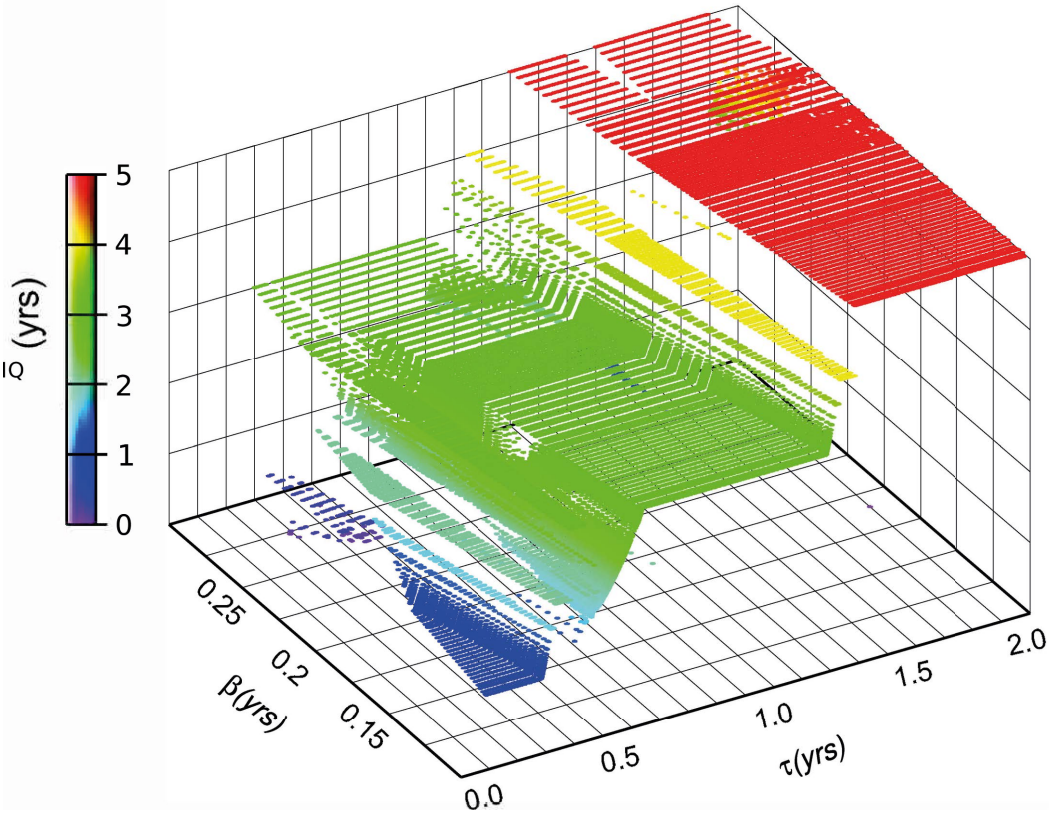

Figure 5. The Devil's bleachers in the BDE model of ENSO. The three-dimensional regime diagram shows the average cycle length $\overline{P}$, portrayed in both height and color, vs. the two delays β and τ. Oscillations are produced even for very small values of the local delay β, as long as $\beta \leq \tau$. Variations in the wave delay τ determine oscillation's period, while changing β establishes the bottom step of the staircase, shifts the location of the steps, and determines their width. Modified after Saudners and Ghil (2001).

Periodic solutions with a single cycle (simple period). In this case, every sequence of events, termed an internal cycle, is completely phase-locked to the seasonal cycle, meaning that warm events always reach their peak at the same time each year. For each fixed value of β, solutions with simple periods of 2, 3, 4, 5, 6, and 7 years arise sequentially, as τ increases; see the large steps in the overall Fig. 4, formed mostly by blue dots that stand for purely periodic solutions.

Periodic solutions with multiple cycles (complex period). In these sequences, several distinct cycles together compose the full period. We describe this by the parameter $\overline{P} = P/n$, where P denotes the total period length and n represents the number of distinct cycles. Notably, as we shift from a three-year period to a four-year period, $\overline{P}$ emerges as a nondecreasing step function of τ that takes only rational values, arranged along a Devil's Staircase; see bottom inset of Fig. 4.

Quasi-periodic (QP) route to chaos in the BDE model. The frequency-locking behavior observed in the BDE model's solutions is a hallmark of the universal QP route to chaos as exemplified by the Arnol'd circle map (Arnol'd, 1983). Indeed, when the nonlinearity is small, this average shift, and hence the average period, is predominantly determined by β; this period may be either rational or irrational, with the latter being more likely due to the ubiquity of irrational numbers. At a critical value of τ only rational periods persist, and a complete Devil's Staircase forms. Beyond this thresh old, chaos ensues, with the system jumping irregularly between resonances (Jensen et al., 1984; Schuster, 1988).

During the transition from an average period of two years to three years, a far more intricate and previously unforeseen structure – the *fractal sunburst* – emerges; see the top inset in Fig. 4. As the wave delay τ increases, mini-ladders begin to form, collapse, or descend, only to ascend again. Around a critical value of $\tau \sim 0.5$ years, these mini-ladders condense rapidly, and the structure becomes self-similar, with each zoom revealing the same pattern on smaller scales. We refer to this as a "bizarre" attractor, as it extends beyond the usual "strange" attractors. While

strange attractors are found in a system's phase space for fixed parameters, this fractal sunburst appears in the phase-parameter space of our model, much like the Devil's Staircase, and it appears to be a remarkable addition to the catalog of fractals (Mandelbrot, 1982; H.-O. Peitgen and Richter, 1986; H. Peitgen et al., 1992).

The combined influence of the local-process delay β and the wave-dynamics delay τ is illustrated in the three-dimensional *Devil's bleachers* – or "Devil's terrace," as termed by Jin et al. (1996) – of Fig. 5. Ghil and Robertson (2000) discussed in greater detail the hierarchy of models outlined in Sec. 1, as applied to the ENSO phenomenon. Jin et al. (1994, 1996) proposed an *intermediate* model this hierarchy, positioned between the simplest "toy models" (BDEs or ODEs) and complex, detailed models based on discretized PDEs in three spatial dimensions, such as the general circulation models (GCMs) employed in the climate simulations of the Intergovernmental Panel on Climate Change (IPCC).

The intermediate model of Jin and colleagues is based on a system of nonlinear PDEs in one spatial dimension, i.e., longitude along the equator. The Devil's bleachers in our BDE model closely resemble those in Jin et al. (1996)'s intermediate ENSO model; see Ghil (2019, Fig. 9). The Jin et al. (1996) model, however, does not exhibit a fractal sunburst, which might be a peculiarity of the BDE model. The main result, though, namely the QP scenario of transition to chaos and the Devil's bleachers, are shared by the low-end and the intermediate model.

Various characteristics of the Devil's Staircase have been well-documented in both observational data (Jiang et al., 1995; Moron et al., 1998; Yiou et al., 2000) and GCM simulations (Ghil and Robertson, 2000; Jin et al., 1994) of ENSO. However, it remains to be seen whether the fractal sunburst will also be found in these cases. If so, it could be linked to the fact that spectral analyses of SSTs and surface winds from the Tropical Pacific frequently reveal a broad peak with a period between two and three years (Rasmusson et al., 1990; Jiang et al., 1995), which is all that might be left of this complex structure in the presence of random perturbations that are due to rapid, small-scale fluctuations.

5. Perspectives on BDEs in the Geosciences

As summarized herein, BDEs represent a powerful mathematical framework for modeling complex dynamical systems, particularly in the geosciences, where interactions often involve time delays and discrete state transitions. As shown in Sec. 1, the principal characteristic of BDEs lies in their ability to simplify intricate processes through the representation of system states as binary variables. This binary representation allows for a clear understanding of the dynamics governing systems like earthquakes and climatic extrema (Ghil et al., 2011), where the state of each component can be classified into discrete conditions, such as "loaded" or "unloaded", "warm" or "cold".

In geophysical systems, BDEs facilitate the modeling of transitions between these states by accounting for various time delays that influence the interaction between components, cf. Section 2. For instance, in the context of seismicity, the delayed transitions are critical as they reflect the accumulation of stress in fault systems and the eventual release of energy during an earthquake event. The BDE framework allows researchers to incorporate feedback mechanisms inherent in geophysical processes, where a change in the state of one element can significantly affect neighboring elements over time.

A BDE model was shown in Section 3 to be particularly well suited for capturing the complexities of seismic cycles, which involve periods of stress accumulation followed by sudden releases of energy, manifested as earthquakes. By integrating concepts from colliding-cascade models, BDEs provide a structure where the interactions among fault lines can be visualized as a directed graph. Each node in this graph symbolizes a fault or stress element, characterized by its state of weakness or fatigue, and its transitions between states are governed by specific time delays. The incorporation of time delays – such as those representing the duration of stress application, failure events, unloading processes, and healing periods – enhances the model's capacity to simulate realistic earthquake sequences, thus yielding synthetic catalogs that mirror actual seismic records.

The application of BDEs has led to significant findings in both seismicity and the dynamics of the El Niño-Southern Oscillation (ENSO). In the case of seismicity, BDEs have demonstrated the ability to reproduce critical features of earthquake dynamics, including the Gutenberg-Richter relation and the clustering of seismic events in space and time. The model identifies different seismic regimes, such as high and nearly periodic seismicity, intermittent seismicity, and medium or low seismicity, thereby providing a framework to analyze transitions between these states. By varying parameters such as time delays and stress loading rates, researchers can observe shifts in seismic behavior, offering insights into the underlying mechanisms that trigger major earthquakes.

For ENSO dynamics, a BDE model effectively captures the complex interactions between sea surface temperature (SST) anomalies and the atmospheric circulation; see Sec. 4. By incorporating delayed responses of atmospheric variables to oceanic states, the BDE framework provides further insights into how positive and negative feedback mechanisms drive the oscillatory nature of ENSO events. The model identifies key variables that influence the system's behavior, such as the strength of trade winds and seasonal forcing, demonstrating how these factors contribute to the regularity and irregularity observed in ENSO cycles. The similarity between the regime diagram of such a simple BDE model in Fig. 5 and the one of a much more conventional and detailed PDE-based model (Ghil, 2019, Fig. 9) is very encouraging in terms of the trustworthiness of the former.

The versatility of BDEs extends beyond seismicity and climate oscillations, offering significant potential for applications in various geophysical phenomena. One of the most pressing areas of interest lies in the modeling of tipping points within the climate system. Tipping points refer to critical thresholds at which a small change in external conditions can lead to drastic shifts in the state of a system, resulting in potentially irreversible changes. In the context of global warming, understanding these tipping points is crucial for anticipating the impacts of climate change on ecosystems, weather patterns, and sea-level rise.

BDEs can be utilized to investigate the transitions between stable and unstable states within the climate system, thereby aiding in the identification of feedback mechanisms that contribute to tipping points. For instance, the melting of polar ice caps can lead to alterations in ocean currents, which may subsequently trigger further warming and additional ice melt – a positive feedback loop that could precipitate a tipping point. By modeling such interactions with BDEs, researchers can simulate scenarios of gradual warming and assess the likelihood of reaching critical thresholds under various emission scenarios.

Additionally, the application of BDEs in modeling transitions between states can provide valuable insights into space weather phenomena, such as geomagnetic storms. These storms arise from solar activity that induces currents in the Earth's magnetosphere, leading to potentially damaging effects on satellites and power grids. By applying BDE modeling to analyze the interactions between solar wind, Earth's magnetic field, and atmospheric conditions, researchers can better understand the conditions that lead to severe geomagnetic events, enhancing predictive capabilities.

Furthermore, as climate systems continue to evolve under global warming, the ability to anticipate critical transitions becomes increasingly important. Elements such as ocean circulation patterns, carbon cycle feedbacks, and biosphere interactions can be modeled using BDEs to uncover the underlying dynamics driving these systems. By identifying early warning signals of tipping points, scientists can inform policymakers and the public about potential future states of the climate, enabling proactive measures to mitigate the impacts of climate change. Considerable interest in early warning signals for such tipping points exists in the literature (Scheffer et al., 2012), and the log-periodic behavior found to be useful in serving this purpose in econophysics for predicting market crashes (Filimonov and Sornette, 2013) might serve similar purposes in the geosciences.

Given the space constraints of this review paper, we have only covered relatively small BDE models that are the counterpart of ODE systems among DDSs, one might say. But BDE systems have been shown to be quite useful on large networks in studying damage propagation (Coluzzi et al., 2011) and on economic networks in studying heterogeneity induced vulnerability and loss of synchronization (Colon and Ghil, 2017). When studying BDEs on large regular lattices, it is the analogy to PDEs that is more useful and one can refer to this study as that of "partial", as opposed to "ordinary", BDEs (Ghil et al., 2008, Sec. 5)

The main results of Coluzzi et al. (2011) and Colon and Ghil (2017) are that delays of unequal length can induce behavior that differs greatly from that of cellular automata or other models where the delays are all equal. Thus, initial damage may propagate or even be amplified, rather than vanish. The effect of network topology and of randomness in the links between nodes and in the delays has also been studied. The Boolean-network approach of Galbusera et al. (2018) can also be relied upon in extending BDE applications from earthquake description and prediction to their impact on built infrastructures.

Next, an interesting aspect of both theory and applications of BDEs is to develop inverse methods. In other words, given the behavior of a complicated natural system, which can be described in a first approximation by a finite, albeit large, number of discrete variables, one would like to discover a good connective linking these variables and yielding the observed behavior for plausible values of the delays. In this generality, the inverse problem for ODEs, say, is clearly intractable. But the asymptotic-simplification results in Sec. 2.2.3, for instance, hold promise for inverse methods to discover and study new systems of BDEs, both in the geosciences and elsewhere. These BDE models, in turn, can suggest more classical and detailed DDS models.

Intuitively, the behavior of BDEs, although surprisingly rich, is more rigidly constrained than that of flows. Certain inverse-modeling successes have been reported for cellular automata; see Wolfram (1994, and references therein). Given today's high level of interest in machine learning and artificial intelligence, with their Boolean variables and structured networks, BDEs may benefit from advances in this area, provide a bridge for understanding their functioning or both.

In conclusion, the application of Boolean Delay Equations in the geosciences and adjacent fields opens up new avenues for understanding and predicting complex interactions. Through their capacity to model delayed state transitions and feedback mechanisms, BDEs provide a robust framework for exploring seismicity, ENSO dynamics, and critical tipping points in the climate system. As the challenges of global warming and climate variability continue to increase, leveraging the insights gained from BDEs will be vital for effective climate mitigation and adaptation strategies.

Data availability statement. No new data have been used in this work.

Acknowledgements. This article is dedicated to the memory of Ilya Zaliapin's scientific and human contributions to our geoscientific community. It is a pleasure to thank Paola Montone for the invitation to participate in this Special Anniversary Issue for the 25th Anniversary of the Italian Istituto Nazionale di Geofisica e Vulcanologia (INGV) and Tommaso Alberti for his editorial advice and encouragement. This paper is ClimTip contribution #22; the Quantifying climate tipping points and their impacts (ClimTip) project has received funding from the European Union's Horizon research and innovation programme under grant agreement No. 101137601. M.G. also received support from the French Agence Nationale pour la Recherche (ANR) project TeMPlex under grant award ANR-23-CE56-1214 0002.

References

Allègre, C. J., J. L. Le Mouel and A. Provost (1982). Scaling rules in rock fracture and possible implications for earthquake prediction, Nature, 297, 47-49.

Arnold, B. H. (1962). Logic and Boolean Algebra. Englewood Cliffs, New Jersey: Prentice-Hall.

Arnold, V. I. (1978). Mathematical Methods of Classical Mechanics, New York: Springer-Verlag.

Arnold, V. I. (1983). Geometrical Methods in the Theory of Ordinary Differential Equations, New York: Springer-Verlag.

Bak, P., C. Tang and K. Wiesenfeld (1988). Self-organized criticality, Phys. Rev. A, 38, 364-374.

Bjerknes, J. (1969). Atmospheric teleconnections from the equatorial Pacific, Mon. Wea. Rev., 97, 163-172.

Bowman, D. D., G. Ouillon, C. G. Sammis, A. Sornettte et al. (1998). An observational test of the critical earthquake concept, J. Geophys. Res., 103, 24359-24372.

Bufe, C. G. and D. J. Varnes (1993). Predictive modeling of the seismic cycle of the greater san francisco bay region, J. Geophys. Res., 98, 9871-9883.

Burridge, R. and L. Knopoff (1967). Model and theoretical seismicity, Bull. Seism. Soc. Am., 57, 341-371.

Chang, P., L. Ji, B. Wang, B. and T. Li (1995). Interactions between the seasonal cycle and El Niño – Southern Oscillation in an intermediate coupled ocean-atmosphere model, J. Atmos. Sci., 52, 2353-2372.

Chang, P., B. Wang, T. Li and L. Ji (1994). Interactions between the seasonal cycle and the Southern Oscillation: Frequency entrainment and chaos in intermediate coupled ocean-atmosphere model, Geophys. Res. Lett., 21, 2817-2820.

Colon, C. and M. Ghil (2017). Economic networks: Heterogeneity-induced vulnerability and loss of synchronization, Chaos: An Interdisciplinary. J. Nonlinear Sci., 27, 12, 126703. doi: 10.1063/1.5017851

Coluzzi, B., M. Ghil, S. Hallegatte and G. Weisbuch (2011). Boolean delay equations on networks in economics and the geosciences, Int. J. Bifurcation Chaos, 21, 12, 3511-3548.

Cowan, G. A. and D. Pines (1994). Complexity: Metaphors, Models and Reality, Reading, Mass: Addison-Wesley.

Darby, M. S. and L. A. Mysak (1993). A Boolean delay equation model of an inter-decadal Arctic climate cycle, Clim. Dyn., 8, 241-246.

Dee, D. and M. Ghil (1984). Boolean difference equations, i: Formulation and dynamic behavior, SIAM J. Appl. Math., 44, 111-126.

Diaz, H. F. and V. Markgraf (1993). El Niño: Historical and Paleoclimatic Aspects of the Southern Oscillation, New York: Cambridge Univ. Press.

Dijkstra, H. A. and M. Ghil (2005). Low-frequency variability of the large-scale ocean circulation: A dynamical system approach, Rev. Geophys., 43, RG3002. doi: 10.1029/2002RG000122

Filimonov, V. and D. Sornette (2013). A stable and robust calibration scheme of the log-periodic power law model. Physica A: Statistical Mechanics and its Applications, 392, 17, 3698-3707.

Gabrielov, A., V. Keilis-Borok, I. Zaliapin and W. I. Newman (2000). Critical transitions in colliding cascades. Phys. Rev. E, 62, 237-249.

Gabrielov, A. M., I. V. Zaliapin, V. I. Keilis-Borok and W. I. Newman (2000). Colliding cascades model for earthquake prediction, J. Geophys. Intl., 143, 427- 437.

Gagneur, J. and G. Casari (2005). From molecular networks to qualitative cell behavior. FEBS Letters, 579 (8), 1867-1871.

Galbusera, L., G. Giannopoulos, S. Argyroudis and K. Kakderi (2018). A Boolean networks approach to modeling and resilience analysis of interdependent critical infrastructures. Computer-Aided Civil and Infrastructure Engineering, 33, 12, 1041-1055. doi: 10.1111/mice.12371

Ghil, M. (2001). Hilbert problems for the geosciences in the 21st century, Nonlin. Processes Geophys., 8, 211-222. doi: 10.5194/npg-8-211-2001

Ghil, M. (2019). A century of nonlinearity in the geosciences. Earth and Space Science, 6, 1007-1042, doi: 10.1029/2019EA000599

Ghil, M. and S. Childress (1987). Topics in Geophysical Fluid Dynamics: Atmospheric Dynamics, Dynamo Theory and Climate Dynamics; reissued as an eBook in 2012. New York/Berlin/London/Paris/Tokyo: Springer Science and Business Media.

Ghil, M. and N. Jiang (1998). Recent forecast skill for the El Niño/Southern Oscillation. Geophys. Res. Lett., 25, 171-174.

Ghil, M. and V. Lucarini (2020). The physics of climate variability and climate change. Rev. Mod. Phys., 92 (3), 035002. doi: 10.1103/RevModPhys.92.035002

Ghil, M. and A. P. Mullhaupt (1985). Boolean delay equations. ii: Periodic and aperiodic solutions. J. Stat. Phys., 41, 125-173.

Ghil, M., A. P. Mullhaupt and P. Pestiaux (1987). Deep water formation and quaternary glaciations. Clim. Dyn., 2, 1-10.

Ghil, M. and A. W. Robertson (2000). Solving problems with GCMs: General circulation models and their role in the climate modeling hierarchy. In D. Randall (Ed.), General Circulation Model Development: Past, Present and Future (pp. 285-325). San Diego: Academic Press.

Ghil, M. et al. (2011). Extreme events: dynamics, statistics and prediction, Nonlin Proces. Geophys., 18, 3, 295-350. doi: 10.5194/npg-18-295-2011

Ghil., M., M. D. Chekroun and G. Stepan (2015). A collection on climate dynamics: multiple scales and memory effects, R. Soc. Proc. A, 470-471.

Ghil, M., I. Zaliapin and B. Coluzzi (2008). Boolean delay equations: A simple way of looking at complex systems, Physica D, 237, 2967-2986, doi: 10.1016/j.physd.2008.07.006

Glantz, M. H., R. W. Katz and N. Nicholls (1991). Teleconnections Linking Worldwide Climate Anomalies, New York: Cambridge Univ. Press.

Guckenheimer, J. and P. Holmes (1997). Nonlinear Oscillations, Dynamical Systems and Bifurcations of Vector Fields (3rd ed.), New York: Springer-Verlag.

Gutowitz, H. (1991). Cellular Automata: Theory and Experiment, Cambridge, MA: MIT Press.

Hale, J. (1971). Functional Differential Equations. New York: Springer-Verlag.

Held, I. M. (2005). The gap between simulation and understanding in climate modeling, Bull. Amer. Meteorol. Soc., 86, 11, 1609-1614.

Jaume, S. C. and L. R. Sykes (1999). Evolving towards a critical point: A review of accelerating seismic moment/energy release prior to large and great earthquakes, Pure Appl. Geophys., 155, 279-306.

Jensen, M. H., P. Bak and T. Bohr (1984). Transition to chaos by interaction of resonances in dissipative systems. Part I. Circle maps, Phys. Rev. A, 30, 1960-1969.

Jiang, N., J. D. Neelin and M. Ghil (1995). Quasi-quadrennial and quasi-biennial variability in the equatorial pacific, Clim. Dyn., 12, 101-112.

Jin, F.-f. (1996). Tropical ocean-atmosphere interaction, the Pacific cold tongue, and the El-Niño-Southern Oscillation, Science, 274, 76-78.

Jin, F.-f., J. D. Neelin and M. Ghil (1994). El Niño on the Devil's Staircase: Annual subharmonic steps to chaos, Science, 264, 70-72.

Jin, F.-f., J. D. Neelin and M. Ghil (1996). El Niño/Southern Oscillation and the annual cycle: Subharmonic frequency locking and aperiodicity, Physica D, 98, 442-465.

Kauffman S. A. (1995). At Home in the Universe: The Search for Laws of Self-Organization and Complexity, New York: Oxford University Press.

Keilis-Borok, V. I. (1994). Symptoms of instability in a system of earthquake-prone faults, Physica D, 77, 193-199.

Keilis-Borok, V. I. (1996). Intermediate-term earthquake prediction, Proc. Natl. Acad. Sci. USA, 93, 3748-3755.

Keilis-Borok, V. I. (2002). Earthquake prediction: State-of-the-art and emerging possibilities, Annu. Rev. Earth Planet. Sci., 30, 1-33.

Keilis-Borok, V. I. and L. N. Malinovskaya (1964). On regularity in the occurrence of strong earthquakes., J. Geophys. Res., 69, 3019-3024.

Keilis-Borok, V. I. and E. Shebalin (1999). Dynamics of lithosphere and earthquake prediction, Phys. Earth Planet. Int., 111, 179-330.

Khinchin, A. Y. (1964). Continued Fractions, Chicago, IL: Univ. of Chicago Press.

Knopoff, L., T. Levshina, V. I. Keilis-Borok and C. Mattoni (1996). Increased long-range intermediate-magnitude earthquake activity prior to strong earthquakes in California, J. Geophys. Res., 101, 5779-5796.

Latif, M. et al. (1994). A review of ENSO prediction studies, Clim. Dyn., 9, 167-179.

Lichtenberg, A. J. and M. A. Liebermann (1992). Regular and Chaotic Dynamics (Second ed.), New York: Springer-Verlag.

Lorenz, E. N. (1963). Deterministic nonperiodic flow, J. Atmos. Sci., 20, 130-141.

Mandelbrot, B. (1982). The Fractal Geometry of Nature, New York: W. H. Freeman.

Maraun, D. and J. Kurths (2005). Epochs of phase coherence between El Niño/Southern Oscillation and Indian monsoon, Geophys. Res. Lett., 25, 171-174.

Mertins, A. (1999). Signal Analysis: Wavelets, Filter Banks, Time-Frequency Transforms and Applications, Chichester: John Wiley and Sons.

Molchan, G. M., O. E. Dmitrieva, I. M. Rotwain and J. Dewey (1990). Statistical analysis of the results of earthquake prediction, based on burst of aftershocks, Phys. Earth Planet. Int., 61, 128-139.

Moron, V., R. Vautard and M. Ghil (1998). Trends, interdecadal and interannual oscillations in global sea-surface temperatures, Clim. Dyn., 14, 545-569.

Mullhaupt, A. P. (1984). Boolean Delay Equations: A Class of Semi-Discrete Dynamical Systems (Unpublished doctoral dissertation), New York University. (Published as Courant Institute of Mathematical Sciences Report CI-7-84, 193 pp.)

Neelin, J. D., M. Latif and F.-f. Jin (1994). Dynamics of coupled ocean-atmosphere models: the tropical problem, Annu. Rev. Fluid Mech., 26, 617-659.

Newman, W. I., A. M. Gabrielov and D. L. Turcotte (1994). Nonlinear Dynamics and Predictability of Geophysical Phenomena, Washington, DC: American Geophysical Union.

Peitgen, H., H. Jurgens and D. Saupe (1992). Chaos and Fractals: New Frontiers of Science. New York: Springer-Verlag.

Peitgen, H.-O. and P. Richter (1986). The Beauty of Fractals. Heidelberg: Springer-Verlag.

Pepke, G. F., J. R. Carlson and B. E. Shaw (1994). Prediction of large events on a dynamical model of fault, J. Geophys. Res., 99, 6769-6788.

Philander, S. G. H. (1990). El Niño, La Niña, and the Southern Oscillation, San Diego: Academic Press.

Rasmusson, E. M., X. Wang and C. F. Ropelewski (1990). The biennial component of ENSO variability, J. Marine Syst., 1, 71-96.

Saunders, A. and M. Ghil (2001). A Boolean delay equation model of ENSO variability, Physica D, 160, 54-78.

Scheffer, M. et al. (2012). Anticipating critical transitions, Science, 338 (6105), 344-348.

Schneider, S. H. and R. E. Dickinson (1974). Climate modeling, Rev. Geophys. Space Phys., 12, 447-493.

Scholz, C. H. (2002). The Mechanics of Earthquakes and Faulting (Second ed.), Cambridge: Cambridge University Press.

Schuster, H. G. (1988). Deterministic Chaos: An Introduction, Weinheim: Physik-Verlag.

Turcotte, D. L. (1997). Fractals and Chaos in Geology and Geophysics (Second ed.), Cambridge: Cambridge University Press.

Turcotte, D. L., W. I. Newman and A. M. Gabrielov (2000). A statistical physics approach to earthquakes. In J. B. Rundle, D. L. Turcotte and W. Klein (Eds.), Geocomplexity and the Physics of Earthquakes, 83-96. Washington, DC: American Geophysical Union.

Tziperman, E., M. A. Cane and S. E. Zebiak (1995). Irregularity and locking to the seasonal cycle in an ENSO prediction model as explained by the quasi-periodicity route to chaos. J. Atmos. Sci., 50, 293-306.

Tziperman, E., L. Stone, M. A. Cane and H. Jarosh (1994). El Niño chaos: Overlapping of resonances between the seasonal cycle and the Pacific ocean-atmosphere oscillator, Science, 264, 72-74.

Varadi, F., B. Runnegar and M. Ghil (2003). Successive refinements in long-term integrations of planetary orbits, Astrophys. J., 592, 620-630.

Wohlleben, T. M. H. and A. J. Weaver (1995). Interdecadal climate variability in the subpolar North Atlantic, Clim. Dyn., 11, 459-467.

Wolfram, S. (1994). Cellular Automata and Complexity: Collected Papers, Reading, Mass: Addison-Wesley.

Yiou, P., D. Sornette and M. Ghil (2000). Data-adaptive wavelets and multi-scale SSA, Physica D, 142, 254-290.

Zaliapin, I., V. Keilis-Borok and M. Ghil (2003a). A Boolean delay equation model of colliding cascades. Part I: Multiple seismic regimes, J. Stat. Phys., 111, 815-837.

Zaliapin, I., V. Keilis-Borok and M. Ghil (2003b). A Boolean delay equation model of colliding cascades. Part II: Prediction of critical transitions, J. Stat. Phys., 111, 839-861.

***CORRESPONDING AUTHOR: Michael GHIL**,
Ecole Normale Superieure and PSL University, Department of Geosciences and Laboratoire de Meteorologie Dynamique, Paris, France
e-mail: ghil@lmd.ipsl.fr